Pb diffusion in magnetite: dating magnetite crystallization and the timing of remanent magnetization in banded iron formation

E. Bruce Watson[1] (watsoe@rpi.edu)

Daniele J. Cherniak[2] (dcherniak@albany.edu)

Claire I. O. Nichols[3] (claire.nichols@earth.ox.ac.uk

B. P. Weiss[4] (bpweiss@mit.edu)

1 - Department of Earth and Environmental Sciences, Rensselaer Polytechnic Institute, 110 Eighth Street, Troy, NY 12180, USA

2 - Ion Beam Laboratory, State University of New York at Albany, 1400 Washington Avenue Albany, NY 12222, USA

3 – Department of Earth Sciences, University of Oxford, 3 South Parks Road, Oxford, UK

4 – Department of Earth, Atmospheric and Planetary Sciences, Massachusetts Institute of Technology, 77 Massachusetts Avenue, Cambridge, MA 02139, USA

Corresponding author: Bruce Watson

This manuscript is paper is a non-peer reviewed preprint submitted to EarthArXiv. This manuscript has been submitted to Chemical Geology for review.

Pb diffusion in magnetite: dating magnetite crystallization and the timing of remanent magnetization in banded iron formation

E. Bruce Watson[1], Daniele J. Cherniak[2], Claire I.O. Nichols[3], Benjamin P. Weiss[4]

[1] Rensselaer Center for Astrobiology Research and Education (RARE) and Department of Earth & Environmental Sciences, RPI, Troy, New York 12180, U.S.A

[2] Department of Physics, University at Albany, State University of New York 12222, U.S.A.

[3] Department of Earth Sciences, University of Oxford, South Parks Road, OX1 3AN, U.K.

[4] Department of Earth, Atmospheric and Planetary Sciences, MIT, Cambridge, Massachusetts 02139, U.S.A.

Abstract

The ferrimagnetic mineral magnetite (Fe_3O_4) is abundant in banded iron formation (BIFs), and has the potential to provide U-Pb or Pb-Pb age information on these rocks because it incorporates small amounts of U during growth. Combined with age measurements, paleomagnetic studies of BIF magnetites may also yield insight into the history of Earth's magnetic field and its relationship to early evolution of Earth's interior and atmosphere.

Reliable magnetite ages utilizing Pb isotopes require knowledge of Pb diffusion in the magnetite structure. For this reason, we undertook an experimental investigation of Pb diffusion in magnetite by diffusing Pb^{2+} ions into pre-polished slabs of natural magnetite oriented parallel to {001} or {111}. A mixture of $PbSO_4$ and Fe_2O_3 was used as a surface powder source to supply Pb^{2+} diffusant at the sample surface and at the same time buffer the oxygen fugacity of the system at magnetite-hematite (MH)—a typical f_{O_2} for banded iron formations (BIFs) due to the common presence of both iron oxides (and where Pb^{2+} is stable relative to other Pb valence states). Diffusion experiments spanned temperatures of 500–675°C and durations of 75 to 2035 h. Following each experiment, in-diffused Pb was depth-profiled using Rutherford backscattering spectroscopy (RBS) and Pb diffusivities were calculated from the profiles using an infinite half-space diffusion model. The following diffusion law for Pb^{2+} in magnetite is based upon 12 independent diffusivity measurements:

$$D_{Pb}\ (m^2 \cdot s^{-1}) = (9 \times 10^{-17}\ m^2 \cdot s^{-1})\ \exp(-98{,}000\ J \cdot mol^{-1})/RT)$$

where the uncertainties in the pre-exponential constant and activation energy are ±6% and ±15%, respectively.

Pb diffusion in magnetite over the temperature range of our study is orders of magnitude slower than projected for other divalent cations based on down-temperature extrapolation of previously measured diffusion laws (e.g., for Mn^{2+}, Fe^{2+}, Co^{2+}, and Ni^{2+}). This finding is encouraging in terms of the potential suitability of magnetite for U-Pb age determinations of BIFs and other magnetite-bearing rocks. Indeed, classical Dodson closure temperatures well above 500°C are not unrealistic in cases where magnetite crystals having large diffusion domains (e.g., >100µm in radius) are cooled relatively rapidly (e.g., at 100°C/MYr). This is of particular significance for paleomagnetic studies, since the Curie temperature of magnetite is 580°C and therefore the age of magnetization in magnetite-bearing rocks may be directly dated. However, slow cooling of magnetites having small diffusion domains can lead to Pb loss at temperatures of 200°C or lower. Pb mobilization is evaluated for various time-temperature scenarios that involve both heating and cooling as well as "closed-loop" time-temperature paths. We conclude that U-Pb or Pb-Pb age determinations of BIF magnetites are potentially reliable, but isotopic results should be assessed in concert with knowledge of the thermal history of the host rock and the effective grain size of the magnetites.

Key words: *magnetite; Pb diffusion; banded iron formation (BIF); remanent magnetization; closure temperature; opening temperature; U-Pb geochronology*

Introduction

Knowledge of Pb diffusion in magnetite crystals from ancient banded iron formation (BIF) is important for several reasons. For example, because BIFs precipitate from seawater under oxidizing conditions, U-Pb (or Pb-Pb) dating of BIF-hosted magnetite can provide time constraints on the oxygenation of the oceans and atmosphere. In addition, because magnetite acquires natural remanent magnetism (NRM) when crystallized in a magnetic field below the Curie temperature (580°C), BIF magnetites may document the existence of an intrinsic terrestrial magnetite field in the deep geologic past. In a broad sense, BIF magnetites have the potential to provide valuable input to the record of Earth's ancient dynamo by shedding light on the timing of thermal and thermochemical remnant magnetization (TRM and TCRM) and the influence of any subsequent thermal overprints. Knowledge of Pb diffusion in magnetite is needed to fully realize this potential in order to understand the relationship between U-Pb age of the magnetite and age of the NRM carried by the magnetite.

Direct age determinations of BIFs can be challenging because these materials generally lack phases well suited to traditional radioisotopic dating techniques. This challenge has led some researchers to evaluate the potential of iron oxides themselves (mainly magnetite [Fe_3O_4] but also hematite [Fe_2O_3]) as candidates for age determinations using the U-Pb or Pb-Pb methods, given that U can be incorporated in these minerals in modest amounts during crystallization. Sufficient concentrations of radiogenic Pb (Pb*) and limited common Pb should enable determination of reliable radiometric ages (Erel at al. 1997; Frei eta l. 1999; Frei and Polat 2007; Courtney-Davies et al. 2022), provided Pb is effectively retained in the magnetite structure following initial crystallization. At the intrinsic oxygen fugacity of metamorphosed BIF (assumed to contain both hematite and magnetite—a solid-state f_{O2} buffer), the stable

oxidation state of lead is Pb^{2+}. No diffusion data for Pb^{2+} in magnetite have been available up to this point, but other divalent cations (e.g., Ni^{2+}, Co^{2+}, Fe^{2+}, Mn^{2+}) are known to diffuse quite fast (leading to closure temperatures of 200-250°C even for mm-sized grains), possibly suggesting poor retention of Pb in magnetite in geologic settings. This prediction is highly uncertain, however, because all existing cation diffusion data were obtained at temperatures in excess of 900°C, which means that large down-temperature extrapolations are needed to address diffusion at temperatures that might have been experienced by a metamorphosed BIF. In addition, the ionic radius of Pb^{2+} is 40-70% larger than those of other divalent cations (e.g., Ni^{2+}, Co^{2+}, Mn^{2+}, Fe^{2+}) whose diffusion laws have been characterized (Van Orman and Crispin 2010)—possibly foretelling more sluggish behavior of Pb^{2+} and better thermal retention in magnetite.

The present contribution describes the results of experiments aimed at characterizing Pb^{2+} diffusion in magnetite over a temperature range of 500° to 675°C, which is directly relevant to the question of Pb retention in natural BIF over geologic time.

Samples and preparation

The magnetite crystals used in this study were from the town of Moriah in eastern Essex County, New York State, obtained from the RPI mineral collection. These crystals are shiny, black octahedra ranging up to ~1 cm in size and containing only minor impurities (see Table 1). They host occasional mineral inclusions, but these were readily avoided during analysis. Slabs of Moriah magnetite 5-8 mm^2 in area and ~1 mm thick were cut with a low-speed diamond saw to obtain slab surface orientations parallel to cubic {001} or octahedral {111} forms. The slabs were polished on one side to produce a surface suitable for in-diffusion of Pb, beginning with 600-grit SiC, progressing to 1 μm alumina powder, and finishing with colloidal silica. This stepwise procedure yielded a polished surface free of dislocations and other lattice damage that

might have been introduced during sample cutting and initial coarse polishing (Watson et al. 2016).

oxide	wt%	σ; *n* = 32
Fe_2O_3	68.59	*
FeO	30.85	*
SiO_2	0.050	0.016
MnO	0.020	0.011
TiO_2	0.105	0.027
Al_2O_3	0.509	0.083
Cr_2O_3	0.01	0.010
MgO	0.10	0.020
V_2O_3	0.01	0.010
NiO	0.01	0.010

* Standard deviation for Fe as FeO = 0.56

Table 1. Moriah magnetite composition determined by electron microprobe (RPI Cameca SX100 operating at 15 kV; 20 nA; 1 μm beam spot). Fe_2O_3/FeO estimated from stoichiometry. Data are averages of two crystals.

Methods

Experimental

The general strategy of the diffusion experiments was to pack the polished magnetite slabs in a Pb-bearing powder that would serve as a source of Pb^{2+} ions at the magnetite surface during high-temperature diffusion anneals. Mechanistically, Pb^{2+} was expected to diffuse into the magnetite in limited exchange for out-diffusing Fe^{2+}. The chosen Pb source was a mixture of $PbSO_4$ and Fe_2O_3 in a mass ratio of 1:1 or 1:2. These two compounds were pre-reacted at 900°C for several hours before use in diffusion experiments; in some cases the Pb diffusion source in a particular diffusion experiment consisted of source powder recycled from an earlier run.

The specific choice of $PbSO_4$–Fe_2O_3 as our powder source was based partly on earlier success in our group using $PbSO_4$ as the source in a study of Pb diffusion in zircon (Cherniak and Watson 2001). In the present case, our use of Fe_2O_3 as the diluent of $PbSO_4$ was strategic in the sense that the coexistence of this compound with the Fe_3O_4 diffusion sample constitutes a solid-state oxygen fugacity buffer (magnetite-hematite, or MH). This was advantageous because most BIFs contain both magnetite and hematite (Klein 2001; Konhauser et al. 2017), and PbO is

111 the stable oxidation state of Pb at the oxygen fugacity of the MH buffer (see Figure 1). Buffer-

112 ing f_{O_2} at MH insured that Pb was generally divalent in our experiments—as would be the case in

113 BIFs—and that uptake of Pb in magnetite would logically take place in exchange for Fe^{2+}.

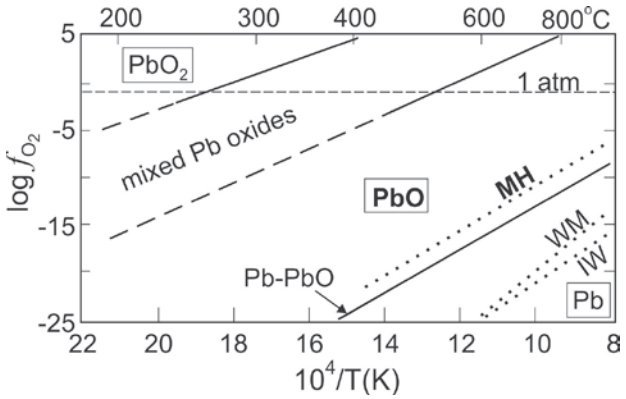

114

Figure 1. Phases in the Pb-O system as a function of temperature and oxygen fugacity. The solid lines delineate the stability fields of Pb-O phases; dashed extensions are estimates beyond the range of direct experimental measurement. The Pb-O data are from White and Roy (1964) and Otto (1966). Also shown as dotted lines are the positions of familiar mineral redox buffer curves in the iron-oxygen system: MH = magnetite-hematite; WM = wüstite-magnetite; IW = iron-wüstite. For the present purposes, the important point is that PbO (i.e., Pb^{2+}) is stable when the oxygen fugacity is buffered at MH, as is the situation in our experiments and most banded iron formations.

115 Diffusion experiments were set up by packing a polished magnetite slab in the Pb source

116 powder inside a 5×7 mm SiO_2 glass tube that had been pre-sealed at one end. The tube was then

117 evacuated and sealed off above the sample with an H_2-O_2 torch, and the length containing the

118 sample was separated from the rest of the tube (by fusion) to create an evacuated ampoule 3-4

119 cm in length with sample and source inside (see Figure 2). A diffusion anneal was conducted by

120 hanging the ampoule in a vertical tube furnace, heating it to a predetermined temperature,

121 holding for a prescribed duration, and quenching the ampoule in air by removal from the furnace.

122 The experiments covered 500° to 675°C, with durations ranging from 75 to 2035 hours (see

123 Table 2). Experiments below 500°C were not practical because of the long duration required to

124 produce measureable Pb uptake in the magnetite. Experiments above 675°C resulted in reaction

125 between the magnetite surface and the Pb source, which compromised the suitability of the

126 surface for measuring diffusive uptake of Pb.

127 Most experiments were conducted on magnetite slabs cut parallel to {001}, but two

128 samples oriented parallel to {111} were also run to confirm the isotropic character of Pb

diffusion in magnetite, which is expected of a crystal belonging to the isometric (cubic) crystal system. A time series of experiments spanning 75-476 hours was conducted at 650°C to establish that the measured Pb diffusivity is independent of experiment duration.

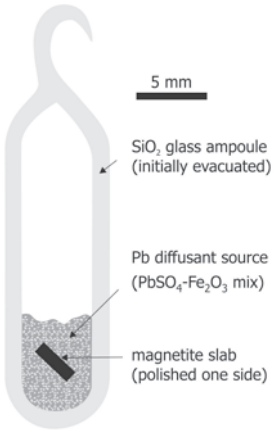

Figure 2. Schematic representation of the container, sample, and source configuration for experiments on Pb diffusion in magnetite. See text for details.

Analytical

Following recovery of the magnetite slabs from air-quenched glass ampoules, they were sonicated in ethanol and evaluated for surface integrity (i.e., lack of obvious reaction with the Pb source) using optical microscopy. The samples were then depth-profiled perpendicular to the polished surface using Rutherford backscattering spectroscopy (RBS) at the Dynamitron accelerator in the Ion Beam Laboratory at the University at Albany (SUNY). RBS is well suited to the present study because the technique is most sensitive for characterization of high-mass impurities in a relatively light matrix. A $^{4}He^{+}$ beam of energy 2 MeV was used for RBS analyses, with a solid-state surface barrier detector used to detect backscattered He. Beam spots were typically about $1mm^{2}$. We achieved a detection limit for Pb of ~50 ppm and a spatial (depth) resolution of ~10 nm. A typical RBS spectrum is presented in Figure 3, where the peak representing in-diffused Pb is seen to be well separated from the Fe edge. Note that the energy of a backscattered He ion (proportional to channel number in the spectrum) depends positively

on the mass of the scattering nucleus and negatively on the depth in the sample at which the scattering event occurs. It is the latter effect that enables depth-profiling for concentration.

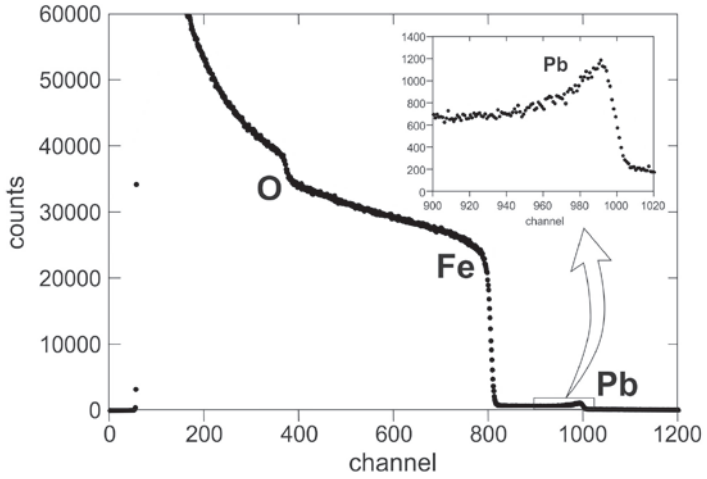

Figure 3. A typical Rutherford back-scattering (RBS) spectrum obtained by depth-profiling a magnetite crystal surface into which Pb was diffused from a surface source (see Figure 2). The Pb feature is small because of the low concentration of Pb, but the enlargement at the upper right reveals the monotonic diminution of Pb progressing into the crystal from the surface at the right. See text for additional RBS details.

The Pb spectral feature is readily converted to a concentration profile (see Cherniak and Watson 2001), two examples of which are shown in Figure 4a & b. Lead diffusivities were extracted from the concentration profiles by invoking the solution to the non-steady state diffusion equation in 1 dimension for the specific case of diffusion into a semi-infinite medium from a planar surface at which Pb concentration remains constant over time. The relevant solution for these boundary conditions is

$$\frac{C(x,t)}{C_0} = 1 - \mathrm{erf}\left(\frac{x}{\sqrt{4D_{Pb}\,t}}\right) \qquad (1)$$

where $C(x,t)$ is the concentration of Pb at distance x from the surface and time t, C_0 is the concentration at the surface, and D_{Pb} is the diffusivity of Pb in the magnetite structure. Concentration versus depth data from RBS analysis of a magnetite slab were inverted through the error function (i.e., by plotting $\mathrm{erf}^{-1}(1\text{-}C/C_0)$ vs. x) to obtain an expected linear array (Figure 4c & d). Linear regression yielded a slope ($= -1/\sqrt{4D_{Pb}\,t}$) and diffusivity from this plot.

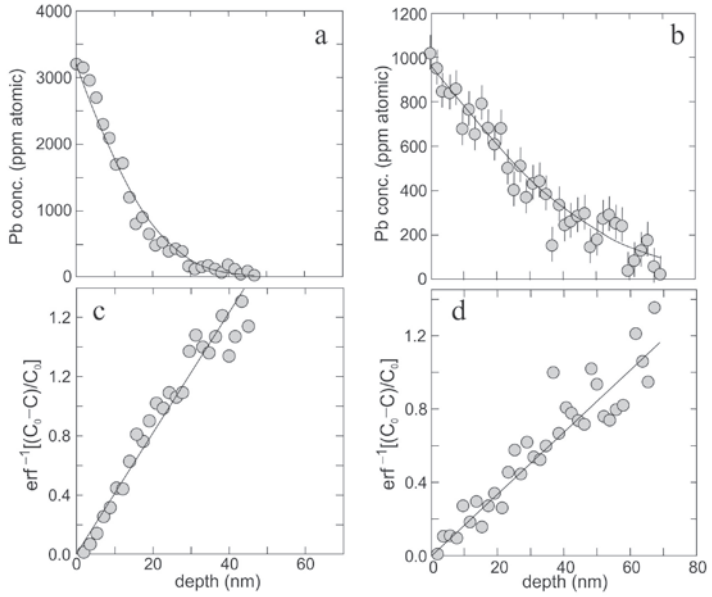

Figure 4. (**a** & **b**) Two examples of Pb "in-diffusion" profiles obtained from experimentally treated magnetite crystals: (**a**) Shows one of the shortest profiles obtained in this study (run PbMt-2); (**b**) is one of the longest (run PbMt-12). The curves are error-function fits to the data, obtained by assuming conformance with equation 1. (**c** & **d**) are linearized versions of **a** & **b**, respectively, in which the raw concentration data have been inverted through the error function. Diffusivities are calculated from the slopes of the linearized data plots, as discussed in the text.

Results and discussion

Data systematics

Lead diffusivities recovered from 12 experiments are listed in Table 2 and plotted in Figure 5, which includes ±1σ uncertainties in D_{Pb} values based upon the slope uncertainties of the raw data plots described above. Least-squares fitting of logD_{Pb} versus reciprocal absolute temperature (T) yields an Arrhenius-type relation:

$$D_{Pb}\,(m^2 \cdot s^{-1}) = D_0 exp[-E_a/RT] \qquad (2)$$

where R is the gas constant. The pre-exponential constant (D_0) has a value of 9×10^{-17} $m^2 \cdot s^{-1}$ (±6%) and the activation energy (E_a) is 98,000 $J \cdot mol^{-1}$ (±15%).

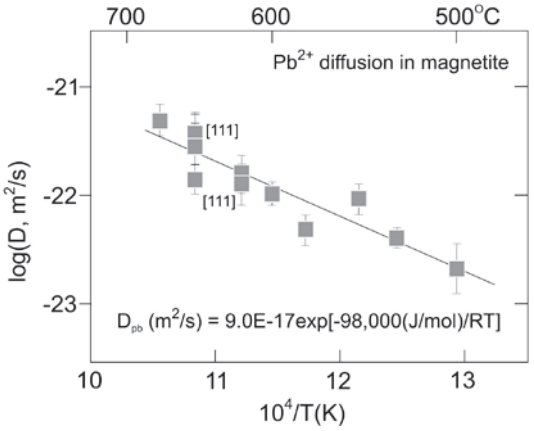

Figure 5. Summary of Pb diffusivities on an Arrhenius-type plot. All measurements except the two labeled {111} involved Pb diffusion perpendicular to {100}. Error bars represent ±1σ uncertainties in the slopes of plots like those shown in Figure 4c & d. See text for discussion and Table 2 for a summary of experiments and results.

172 **Table 2**. Summary of Pb diffusion experiments and results

Expt. No.	T(C)	time (h)	D (m^2/s)	logD	σ
PbMt-2	600	405	1.03×10^{-22}	-21.99	0.13
PbMt-3	500	2035	2.09×10^{-23}	-22.68	0.27
PbMt-4	675	94	5.00×10^{-22}	-21.30	0.17
PbMt-5	550	815	9.33×10^{-23}	-22.03	0.16
PbMt-8a	620	331	1.60×10^{-22}	-21.80	0.20
PbMt-8b	620	331	1.24×10^{-22}	-21.91	0.22
PbMt-10	650	260	3.90×10^{-22}	-21.41	0.22
PbMt-11	580	1200	4.81×10^{-23}	-22.32	0.17
PbMt-12	530	1179	4.00×10^{-23}	-22.40	0.11
PbMt14a	650	74.5	2.88×10^{-22}	-21.54	0.37
PbMt-15a	650	476	1.27×10^{-22}	-21.90	0.16
PbMt-15b	650	476	3.84×10^{-22}	-21.42	0.13

173

174 Figure 6 shows four Pb diffusivities resulting from a time series of experiments
175 conducted at 650°C. Three values from experiments of 75, 260 and 476 h duration are
176 indistinguishable within uncertainty. The value obtained from a separate 476-h experiment is
177 slightly low relative to the other three, but is nevertheless in agreement at the ±2σ level.
178 Importantly, there is no suggestion of systematic time dependence of the data, which is
179 consistent with Pb transport in magnetite by volume diffusion.

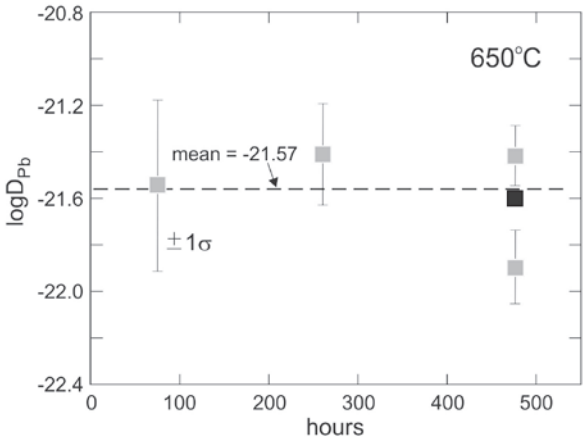

Figure 6. Lead diffusivities resulting from a series of experiments of varying duration conducted at 650°C. The lack of time dependence is indicative of diffusion control of Pb transport. The black square is the average of the two experiments of the same duration.

180

181 In Figure 7, results for Pb diffusion in magnetite are shown in comparison with diffusion
182 laws from the literature for Al, Ti, Cr, Mn, Fe, Co and Ni in magnetite (Van Orman and Crispin

2010), all characterized at an f_{O_2} corresponding to MH. The previous studies were conducted at much higher temperatures than the present investigation, so detailed comparison of diffusion relationships is of limited value. However, down-*T* extrapolation of published Arrhenius laws to the ~500-700°C range of our study suggests diffusivities for most cations that are orders of magnitude higher than that of Pb. Chromium is a possible exception; in this case—because E_a for Cr diffusion is relatively high—down-T extrapolation places Cr diffusivities in the vicinity of our Pb values at 500-600°C. Note that the activation energy for Pb diffusion (98 kJ/mole) is quite low relative to E_a for other cations. This raises the possibility that an extrinsic (defect-related) diffusion mechanism is in play for Pb, which would make up-temperature extrapolation of our Arrhenius law beyond the range of measurements somewhat risky. Fortunately, the temperature range of many geologic applications (including those involving BIFs) falls within or below the temperature span of our experiments (see next section)..

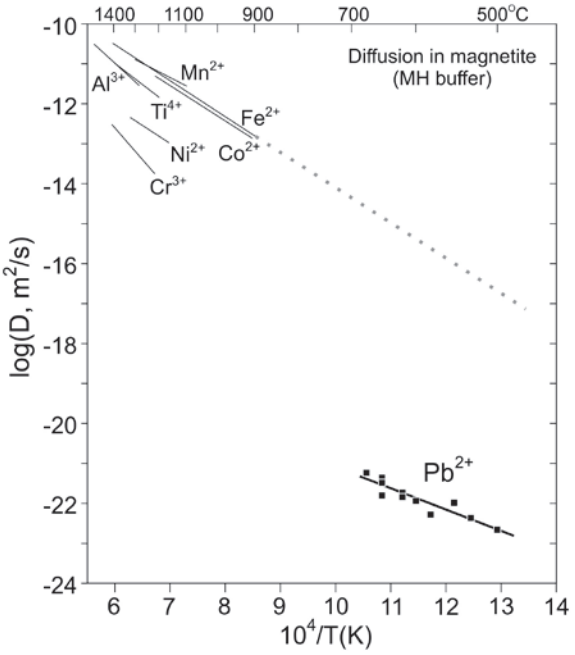

Figure 7. Diffusion data from the literature (upper left) compared with present measurements for Pb (lower right). All data were obtained at oxygen fugacities corresponding to the MH buffer. With the possible exception of Cr, down-temperature extrapolation of most Arrhenius laws to 500-700°C indicates diffusivities much higher that than of Pb. The Fe^{2+} line is extended to low temperature (gray dotted line) to emphasize that Pb-Fe interdiffusion is probably not rate-limited by Fe in our experiments. See Van Orman and Crispin (2010) for data sources.

A useful conclusion from Figure 7 is that Fe diffusion in magnetite at the temperatures of our experiments (estimated by down-T extrapolation) is 5-6 orders of magnitude faster than Pb

198 diffusion. If, as we suspect, Pb^{2+} diffuses in magnetite by exchange with Fe^{2+}, it seems clear that
199 Pb-Fe interdiffusion is not rate-limited by Fe mobility.
200 *Pb retention in magnetite: diffusive closure and opening*
201 Equipped with an Arrhenius relation for Pb diffusion in magnetite, we can now evaluate
202 the retention of radiogenic Pb in natural magnetite crystals subjected to geologic cooling, heating
203 or thermal cycling. The usual first step in such an assessment is to calculate (by iteration) the
204 closure temperature (T_C) according to the formula of Dodson (1973):

205
$$T_C = \frac{E_a / R}{\ln\left[\frac{55RT_c^2(D_0/a^2)}{E_a(dT/dt)}\right]} \qquad (3)$$

206 where E_a, R and D_0 are as defined for equation 2, a is the radius of the diffusion domain, dT/dt is
207 the cooling rate, and the constant 55 is a geometrical factor specific to a spherical diffusion
208 domain. In principle, the diffusion domain for natural magnetites could be the entire crystal, but
209 it is also possible that the domain is smaller due to the presence of fast diffusion pathways in the
210 crystal. We note that the diffusion domain as defined here has no relationship to the magnetic
211 domain state of the magnetite. The latter property reflects whether a grain is homogenously
212 magnetized (single domain, which occurs for grains <~60 nm in diameter) or non-uniformly
213 magnetized (pseudo single domain and multi-domain, which occurs for larger grains; [Nagy et
214 al. 2017]).
215 The closure temperature given by equation (3) applies strictly to cooling regimes in
216 which temperature decreases at geologic rates in inverse proportion to time (e.g., as a banded
217 iron formation cools after attaining peak metamorphic conditions). Figure 8 shows T_C as a
218 function of diffusion domain size and cooling rate. For large diffusion domain radii of 1 mm or
219 greater, T_C can be as high as ~800°C for rapidly-cooled systems (e.g., at 100°C/MYr), but drops

dramatically at slow cooling rates (e.g., 1°C/MYr) and for smaller diffusion domain sizes that might better reflect those of some BIF magnetites. For diffusion domain radii on the order of 1 μm, for example, closure does not set in during cooling until the system reaches 150-200°C. Nichols et al. (in prep.) estimated the diameters of magnetite grains in Isua BIF samples to fall in the range 1-27 μm. At the upper end of this size range, T_C is ~380°C for cooling at 100°C/MYr. This is well below the 580°C Curie temperature for magnetite, which means that a Pb-Pb or U-Pb age determination could be more recent than the acquisition time of NRM. However, it still serves as a useful age for any subsequent thermal overprints that may have influenced the NRM after initial acquisition (see final section).

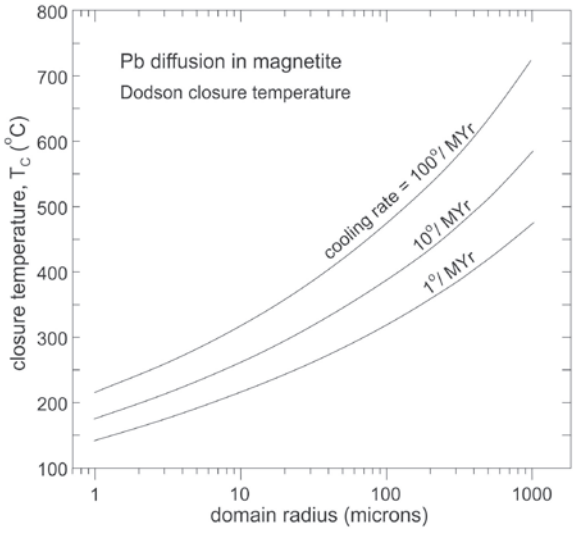

Figure 8. Closure temperature (T_C) for Pb diffusion in magnetite as a function of cooling rate and diffusion domain radius, according to the Dodson formulation (equation 3 in text). See text for discussion.

Diffusive closure during cooling as described by the Dodson equation may be of limited usefulness for many BIFs because these rocks represent metamorphosed sediments that have experienced a thermal cycle. Magnetite grains in BIFs are generally believed to have crystallized under diagenetic or low-grade metamorphic conditions (Rasmussen and Muhling 2018; Konhauser et al. 2017; Nutman 2017) where Pb is effectively immobile. However, partial or total open-system behavior of Pb could set in at any point during prograde metamorphism, which would greatly complicate the interpretation of U-Pb data. A protocol for assessing Pb mobility

237 throughout a metamorphic cycle is essential, perhaps especially at temperatures near the
238 magnetite Curie point.

239 The risk of relying on T_C to rule out diffusive loss during heating is starkly illustrated by
240 the fact that 40% diffusive loss is the inevitable result of linear heating from ambient temperature
241 up to Dodson's T_C (Cherniak and Watson 2007; Watson and Cherniak 2013). Such loss would
242 result in an underestimate of age, and might not be recognizable on a Concordia diagram because
243 of its gradual nature. Fortunately, diffusive loss can be quantified for any heating scenario if the
244 Arrhenius law (E_a and D_0) for the diffusant of interest is known. Cherniak and Watson (2007)
245 and Gardés and Montel (2009) provided equations that describe diffusive opening in a manner
246 broadly analogous to that of Dodson (1973) for closure during cooling. Watson and Cherniak
247 (2013) presented, in addition, a general equation that gives the specific extent of diffusive loss
248 during linear heating to any temperature of interest. For linear heating ($T \propto$ time), diffusive
249 opening is described by

$$T_{rt\%} = \frac{0.457 \cdot (E_a / R)}{\chi_h + \log\left[\frac{E_a \cdot D_0}{R \cdot dT/dt \cdot a^2}\right]} \quad (4)$$

250

251 where $T_{rt\%}$ is the temperature (in kelvins) at which a specific fractional retention occurs, which
252 coincides with a specific value of the constant χ_h. For example, χ_h has a value of 2.756 for 99%
253 retention during heating; χ_h values for retention levels ranging from 0.1 to 99.9% are provided in
254 Watson and Cherniak (2013). Figure 9 shows temperatures corresponding to 50, 80, 99 and
255 99.9% retention of Pb as a function of diffusion domain size at linear heating rates of 10° and
256 100°/MYr. Note that 99% Pb retention (1% diffusive loss) occurs at ~350°-375°C for 1-μm
257 diffusion domains and ~575°-650°C for 1-mm diffusion domains (see Fig. 9b). A substantial

fraction of Pb is retained to considerably higher temperatures (see 80% and 50% curves in Figs.9c and 9d), but the U-Pb isotopic system is clearly compromised in these cases.

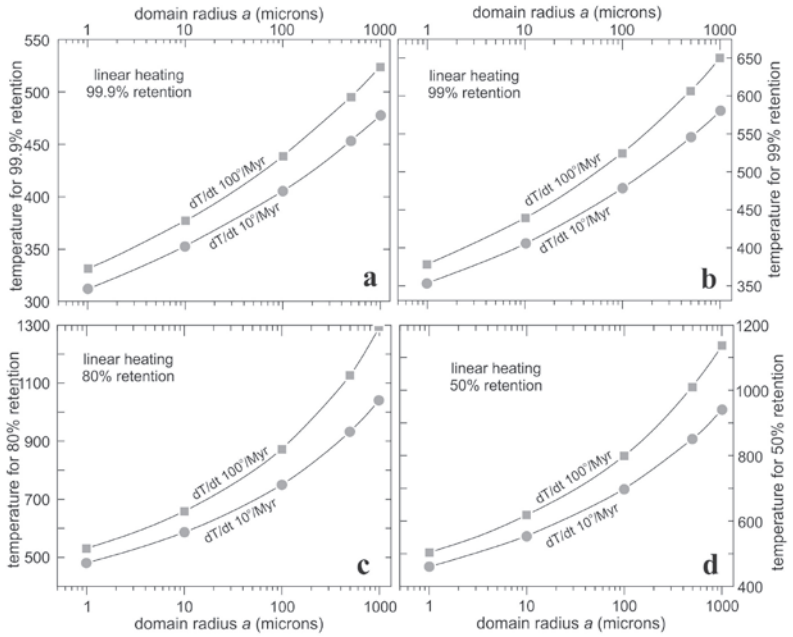

Figure 9. Diagrams illustrating diffusive opening of Pb in magnetite as a consequence of heating ($T \propto t$) at rates of 10 and 100°C/MYr. The plotted temperatures correspond to 99.9, 99, 80 and 50% Pb retention, respectively, in panels a, b, c, and d. Note the strong dependence of opening behavior upon the radius of the diffusion domain. These plots were generated using equation 4; see text for details and discussion.

In the context of BIF thermal evolution, the most relevant diffusive opening scenarios might be closed-loop events (i.e., complete thermal cycles that include both prograde and retrograde metamorphism). Watson and Cherniak (2013) developed general equations that can be used to calculate the extent of diffusive loss during such events, including linear heating followed immediately by linear cooling (a "steeple" time-temperature path), as well as parabolic *t*-*T* paths. Here we briefly consider the parabolic case. Fractional loss over a parabolic time-temperature path can be obtained from the following relationship:

$$\log\zeta = \log\left[\frac{D_0\tau}{a^2}\right] + \frac{140}{T_{pk}} - \frac{0.437E_a}{RT_{pk}} - 0.8 \qquad (5)$$

where $\zeta = a^{-2}\int_{t=0}^{\tau} D(t)dt$, τ is the duration of the heating event (in seconds) and T_{pk} is the peak temperature in kelvins (see Figure 10 inset). The total fractional loss (F) is uniquely determined by the value of ζ; conversion of $\log\zeta$ to F is straightforward using tabulated or graphical information found in Watson and Cherniak (2013). Figure 10 shows fractional Pb loss as a

function of T_{pk} and diffusion domain size during a parabolic thermal event lasting 30 MYr. For a diffusion domain radius of 1 mm, total Pb loss is negligible for $T_{pk} \approx 200$°C and ~8% for $T_{pk} \approx$ 400°C. Smaller diffusion domain sizes lead to more significant Pb loss over the same parabolic thermal event. For example, 10 μm diffusion domains result in ~8% Pb loss for a modest peak temperature of 170°C.

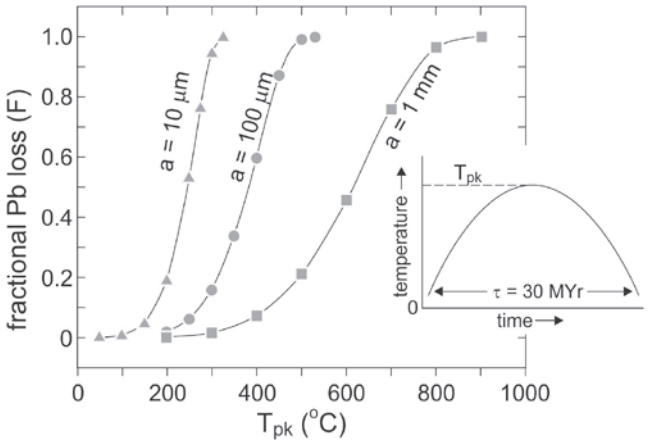

Figure 10. Fractional loss of Pb from magnetite as a function of the peak temperature (T_{pk}) achieved during a 30-MYr parabolic heating event, computed using equation 5. See *T-t* inset and text for discussion.

We note in closing this section that in-growth of Pb is not taken into account by any of the equations used to assess diffusive closure and opening. In-growth of Pb would be minimal over the time scales considered above, so this particular shortcoming will be relatively minor for most BIF *t-T* scenarios. A far greater concern is the lack of constraints on the radius (a) of diffusion domains in natural magnetite crystals. Because the overall diffusive response depends upon a^2, this parameter has a large effect on closure and opening systematics (see Figures 8-10). This limitation is particularly vexing due to the added complication of possible time dependence of the diffusion domain radius during a thermal event of interest. For example, general coarsening of magnetite grains during prograde metamorphism might tend to increase the diffusion domain size over time, improving Pb retention. Stress-induced deformation, on the other hand, could have the opposite effect by introducing defects into the magnetite crystal

290 structure that could serve as fast paths for diffusion, decreasing the effective size of Pb diffusion
291 domains and jeopardizing Pb retention.

292 *Dating BIFs and the timing of NRM acquisition*

293 The challenges above aside, it is instructive to consider the interplay of Pb diffusion
294 behavior and the acquisition and subsequent thermal overprinting of NRM over some
295 hypothetical BIF time-temperature histories. This topic is especially interesting given the great
296 age of some BIFs and the possibility that such rocks might document the early existence of an
297 intrinsic terrestrial magnetic field (Nichols et al. in prep.). Figure 11 illustrates four broadly
298 parabolic time-temperature paths beginning with BIF precipitation in the deep geologic past. In
299 due time the newly-formed BIF is heated (through burial) to a hypothetical peak temperature and
300 then cooled back to Earth's surface temperature (through uplift and erosion) over an unspecified
301 time interval. Because the Pb diffusion domain size is unknown, the opening temperatures are
302 also hypothetical and are deliberately varied among the four scenarios considered. In cases 1-3,
303 magnetite is assumed to be present from its diagenetic origin onward, with implicit coarsening
304 throughout the cycle. In case 4, magnetite crystallization is delayed until mid-metamorphic
305 grade on the prograde limb, at which time coarse crystals are formed.

306 Case 1 in Figure 11 is the simplest of the four scenarios because the peak temperature
307 exceeds neither the opening temperature for Pb diffusion in magnetite nor its Curie temperature.
308 In this case, a U-Pb or Pb-Pb age determination would reflect the formation age of the BIF, and
309 the highest blocking temperature fraction of the NRM carried by single domain magnetite could
310 provide a record of the existence of a terrestrial magnetic field at that time.

311 Case 2 in Figure 11 is more complicated because the diffusive opening temperature for
312 Pb is exceeded as the BIF progresses along its hypothetical *t*-*T* path. The severity of Pb loss

313 could be assessed based on assumed values of the parameters in equation 5, but any amount of
314 Pb loss would only allow a lower limit on the BIF deposition age. Ultimately, the diffusively-
315 compromised BIF cools through the Dodson closure temperature (T_C), and it is this event that a
316 radioisotopic age would reflect. An additional feature of Case 2 is that the Curie temperature of
317 magnetite is not exceeded, so detected NRM could have been acquired during diagenetic
318 magnetite growth shortly after BIF precipitation. This case illustrates the interesting possibility
319 that NRM acquisition could predate the apparent radiometric age of a BIF, and the radiometric
320 age would correspond to a low temperature overprint that can be effectively removed during
321 thermal demagnetization for single-domain magnetite grains.

322 The third hypothetical *t-T* path (Case 3 in Figure 11) considers a BIF containing
323 diffusively retentive magnetite—attributable, perhaps, to the presence of large diffusion domains
324 and/or rapid heating. For the *t-T* path shown, the Curie temperature of magnetite is exceeded but
325 the opening temperature for Pb diffusion is not. The radiometric age of magnetite from this
326 sample would reflect the actual deposition age of the BIF, but NRM present in a recovered
327 sample would have been acquired later as the rock cooled back through the Curie temperature.

328 Our final *t-T* scenario (Case 4 in Figure 11) differs from the previous three in that
329 crystallization of magnetite—rather than being diagenetic—is delayed until intermediate-grade
330 metamorphic conditions are achieved. This case is both plausible and interesting because the
331 resulting magnetite crystals can be assumed to be relatively large and therefore more retentive of
332 Pb than low-T precipitates. Given the existence of a terrestrial magnetic field, NRM would be
333 imprinted at the time of magnetite growth. If radiogenic Pb is fully retained and the Curie
334 temperature is not exceeded, the measured age would accurately reflect the initial BIF
335 metamorphism *and* the existence of a terrestrial magnetic field.

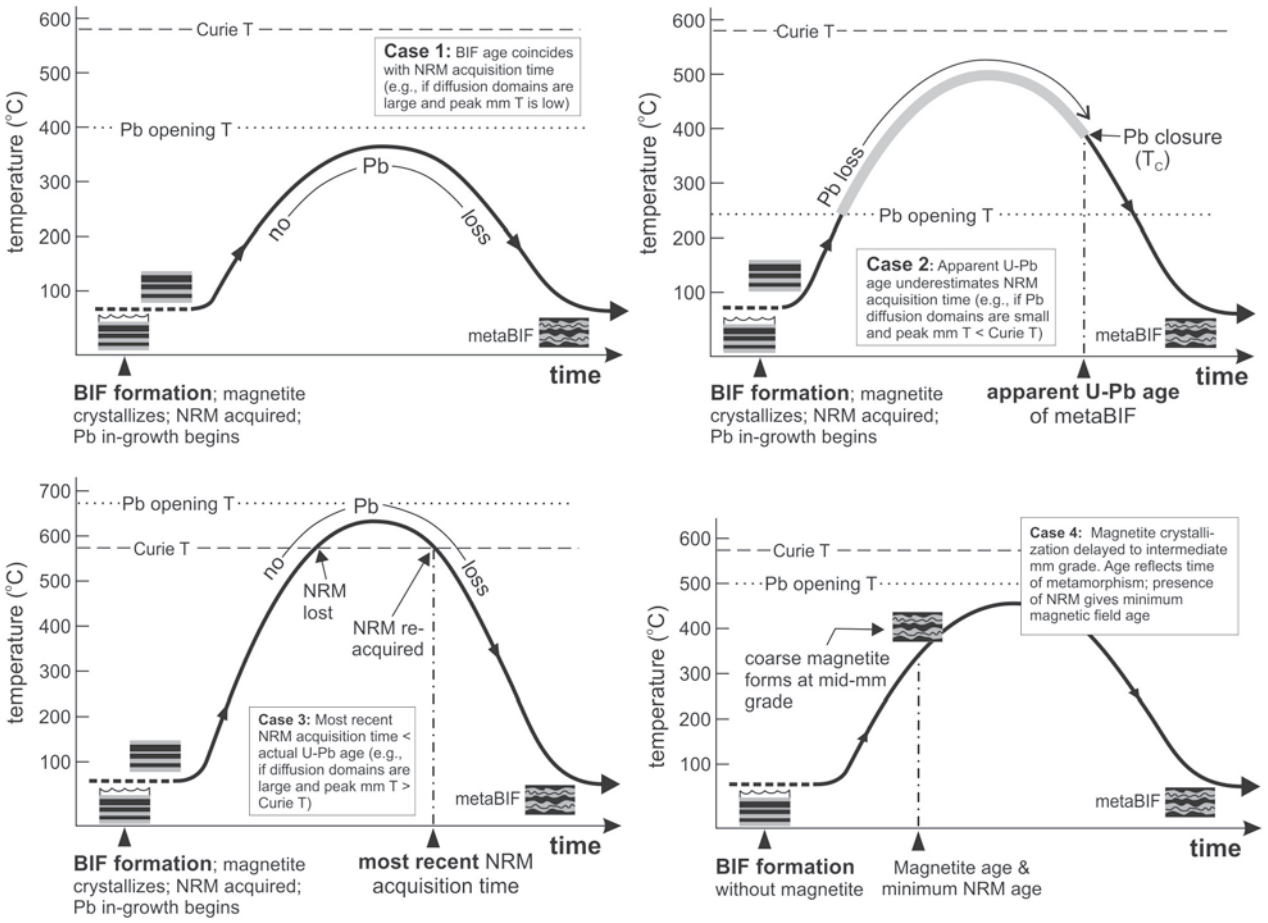

Figure 11. Four time-temperature scenarios illustrating the possible interplay between the Curie temperature of magnetite and opening/closure with respect to Pb diffusion. In cases 1-3 magnetite is assumed to form during BIF precipitation; in case 4, magnetite crystallization is delayed to intermediate metamorphic grade where large crystals are formed. The Pb opening temperature differs among these cases because it depends upon diffusion domain size. See text for discussion.

Based on our new Pb diffusion law, all four time-temperature scenarios illustrated in Figure 11 represent plausible relationships between the Curie temperature and diffusion of radiogenic Pb in BIF magnetite. These examples are not exhaustive, and readers will certainly identify additional possibilities. The crucial realization is that many realistic geologic *t-T* paths can preserve true BIF ages as well as the initial NRM acquisition, but well-constrained estimates of the duration and peak temperature of BIF metamorphism are key to evaluating any natural situation. Also, as noted previously, the size of Pb diffusion domains in magnetite is a crucial

346 factor in Pb retention. The study of Isua BIF by Nichols et al. (in prep.) suggests consistency
347 between the actual grain size of magnetite crystals and the size of Pb diffusion domains, which is
348 another promising indicator of the usefulness of BIF magnetite in studies of the early history of
349 our planet.

350 The main conclusion of this study is that Pb^{2+} diffusion in magnetite is substantially
351 slower than might be inferred from previous data for other cations. This finding is encouraging
352 in terms of the potential for BIF magnetites to yield reliable U-Pb age information, which in
353 some cases will be relatable to paleomagnetic measurements. It must be acknowledged that
354 some geologic scenarios are conducive to open-system behavior of Pb in magnetite and resetting
355 of radioisotopic ages; however, our diffusion law provides a basis for distinguishing between
356 promising and less promising situations. The exciting aspect of our results is that the classical
357 Dodson closure temperature (T_C) for realistic diffusion domain sizes and cooling rates is
358 fortuitously close to the 580°C Curie point of magnetite, which makes the U-Pb system a unique
359 and potentially powerful tool for dating BIF magnetites and the initiation of Earth's dynamo.

360 **Acknowledgements**. BPW and CION are grateful for the support of the Heising-Simons Foundation
361 through grant no. 556352. EBW and DJC acknowledge Rensselaer Polytechnic Institute for contributing
362 analytical costs at the Ion Beam Laboratory at the University at Albany. Oliver Wolfe and Jen Gorce
363 kindly provided the EPMA analyses of the Moriah magnetite.

364

References

D.J. Cherniak, E.B. Watson (2001) Pb diffusion in zircon. Chem. Geol. 172: 5-24.

D.J. Cherniak, E.B. Watson (2007) Ti diffusion in zircon. Chemical Geology 242: 473-486.

L. Courtney-Davies, M. Danisik, E.R. Ramanaidou, C.L. Kirkland, N.J. Evans, A.M. Piechocka, B.I.A. McInnes (2022) Hematite geochronology reveals a tectonic trigger for iron ore mineralization during Nuna breakup. Geology 50: 1318-1323.

M.H. Dodson (1973) Closure temperature in cooling geochronological and petrological systems. Contributions to Mineralogy and Petrology 40: 259-274.

Y. Erel, Y. Harlavan, M. Stein, J.D. Blum 91997) U-Pb dating of Fe-rich phases using a sequential leaching method. Geochim Cosmochim Acta 61: 1697-1703.

R. Frei, D. Bridgwater, M.Rosing, O. Stecher (1999) Controversial Pb-Pb and Sm-Nd isotope results in the early Archean Isue (West Greenland) oxide iron formation: Preservation of primary signatures versus secondary disturbances. Geochim Cosmochim Acta 63: 473-488.

R. Frei, A. Polat (2007) Source heterogeneity for the major components of 3.7 Ga Banded Iron Formations (Isua Greenstone Belt, Western Greenland): Tracing the nature of interacting water masses in BIF formation. Earth Planet. Sci. Lett. 253: 266-281.

E. Gardés, J.-M. Montel (2009) Opening and resetting temperatures in heating geochronological systems. Contributions to Mineralogy and Petrology 158: 185-195.

C. Klein (2001) Presidential address to the Mineralogical Society of America, Boston, November 6, 2001: Some Precambrian Banded Iron-Formations (BIFs) from around the world: Their age, geologic setting, mineralogy, metamorphism, geochemistry, and origin. American Mineralogist 90: 1473-1499.

K.O. Konhauser, N.J. Planavsky, D.S. Hardisty, L.J. Robbins, T.J. Warchola, R. Haugaard, S.V. Lalonde, C.A. Partin, P.B.H. Oonk, H. Tsikos, T.W. Lyons, A. Bekker, C.M. Johnson (2017) Iron formations: A global record of Neoarchaean to Palaeoproterozoic environmental history. Earth-Science Reviews 172: 140-177.

L. Nagy, W. Williams, A. R. Muxworthy, V. P. Shcherbakov (2017) Stability of equidimensional pseudo–single-domain magnetite over billion-year timescales. Proc. Nat. Acad. Sci. 114(39): 10356-10360

C.I.O. Nichols, B.P Weiss, A. Eyster, C.R. Martin, A.C. Maloof, N.M. Kelly, M.J. Zawaski, S.J. Mojzsis, T. Greenfield, E.B. Watson, D.J. Cherniak (2023) An Eoarchean record of the geomagnetic field preserved in the Isua Supracrustal Belt, Southwest Greenland. To be submitted to Proc. Nat. Acad. Sci., June 2023.

A.P. Nutman (2017) Isua stromatolites – Understanding the Field Setting. Technical Report, University of Wollongong. https://doi. org/10.13140/RG. 2.2. 13602.63681.

E.M. Otto (1966) Equilibrium pressures of oxygen over oxides of lead at various temperatures. J. Electrochem. Soc. 113: 525-527.

B. Rasmussen, J.R. Muhling (2018) Making magnetite late again: Evidence for widespread magnetite growth by thermal decomposition of siderite in Hamersley banded iron formations. Precambrian Res. 306: 64-93.

J.A. Van Orman, K.L. Crispin (2010) Diffuson in oxides. Rev. Mineral. Geochem. 72: 757-825.

E.B. Watson, D.J. Cherniak (2013) Simple equations for diffusion in response to heating. Chem. Geol. 335: 93-104.

E.B. Watson, D.J. Cherniak, J.B. Thomas, J.M. Hanchar, R. Wirth (2016) Crystal surface integrity and diffusion measurements on Earth and planetary materials. Earth Planet. Sci. Lett. 450:346-354, DOI: 10.1016/j.epsl.2016.06.043.

W.B. White, R. Roy (1964) Phase relations in the system lead-oxygen. J. Am. Ceram. Soc. 47: 242-249.